Covering glass microspheres with Al_2O_3 or AlN by low-temperature atomic layer deposition

Rafał Stankiewicz[1], Anna Piątkowska[1]

Thin layers of Al_2O_3 and AlN were deposited on the surface of borosilicate glass microspheres in an ALD reactor at 50 and 150°C, respectively. They were imaged by SEM microscopy. X-ray EDS spectroscopy was used to assess chemical composition but it was also the basis for a thickness determination method. Al_2O_3 layers between 20 and 100 nm were obtained, with a constant growth rate of 1.2 Å per deposition cycle. AlN formed continuous but always very thin films on the spheres, generally 5 to 10 nm, even if it was growing much thicker on control glass slides, at 0.8 Å per cycle.

Key words: ALD, EDS, dielectric layers, glass microspheres

Pokrywanie mikrosfer szklanych Al_2O_3 lub AlN metodą niskotemperaturowego osadzania warstw atomowych

W reaktorze ALD osadzano cienkie warstwy Al_2O_3 i AlN na mikrosferach ze szkła borokrzemowego w temperaturach odpowiednio 50 i 150°C. Obrazowano je przy pomocy skaningowego mikroskopu elektronowego. Spektroskopia rentgenowska EDS była wykorzystywana do badania składu chemicznego, ale stanowiła także podstawę dla metody wyznaczania grubości warstw. Otrzymano warstwy Al_2O_3 o grubościach od 20 do 100 nm przy stałej szybkości wzrostu 1,2 Å/cykl. AlN tworzył natomiast ciągłe, lecz zawsze bardzo cienkie warstwy (zwykle 5 do 10 nm), mimo że na kontrolnych płytkach szklanych uzyskiwano znacznie większe grubości, a szybkość wzrostu wynosiła 0,8 Å/cykl.

Słowa kluczowe: ALD, EDS, warstwy dielektryczne, mikrosfery szklane

1. Introduction

Micro-scaled glass spheres or beads are an industrially made product with numerous applications [1]. They can serve as a filler in chemicals, paper [2] and synthetic materials [3] or as a spacer in adhesives [4]. They can also be used for shot peening of various surfaces. When incorporated in paints, coatings and mortar, they improve durability, provide thermal insulation and enhance the surface aspect [5 - 8]. In such substances, spheres can diffuse, refract or reflect light, the latter being particularly important for road marking paints [9]. The optical or decorative effect can be modified by employing glass microspheres coated with thin layers of other materials.

Oxide-coated beads are used in a number of unrelated applications. For instance, layers of SnO_2 and TiO_2 are photocatalysts [10], the latter being used for water decontamination [11, 12]. PbO_2 can serve as an additive for lead acid batteries [13], while $CoFe_2O_4$ has interesting magnetic properties [14] and is also a strong microwave absorber [15]. Such layers are deposited on the spheres by different chemical methods, such as the sol-gel method [10, 12], electroless deposition [13], the coprecipitation method [14 - 15] or chemical vapor deposition [11].

Atomic layer deposition (ALD) is a penetrating and self-limiting deposition technique, appropriate for obtaining thin uniform layers of chemical compounds on arbitrarily shaped surfaces. It is widely employed to deposit dielectric layers in the fabrication of semiconductor devices. Among the materials commonly deposited by ALD, aluminum oxide (Al_2O_3) is used, for example, as the gate oxide in field-effect transistors and aluminum nitride (AlN) can be used in piezoelectric devices or as a passivation layer. Both materials can also serve as antireflective layers. Typically, substrate temperatures of the order of 300°C are used for their deposition. It is possible, however, to adapt such processes to much lower temperatures [16], which extends the range of possible substrate materials (e.g. to glass). In the present work, we investigated if a controlled and uniform deposition can still be achieved if flat substrates are replaced with a pile of glass microspheres.

2. Experimental

Dielectric layers were deposited on borosilicate glass spheres, with different diameters present in each sample, ranging from a few micrometers to over 200 μm (Fig. 1), but mostly comprised between 20 and 150 μm. Visually, the spheres were forming a fine white powder. Their wall

[1] *Institute of Electronic Materials Technology*, 133 Wólczyńska Str., 01-919 Warsaw, Poland, e-mail: rafal.stankiewicz@itme.edu.pl

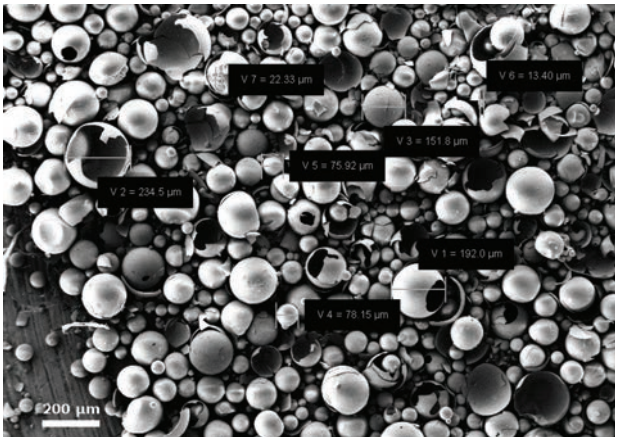

Fig. 1. Glass microspheres imaged by scanning electron microscopy. The diameters of selected spheres were measured.
Rys. 1. Obraz mikrosfer szklanych ze skaningowego mikroskopu elektronowego (SEM). Zmierzono średnice wybranych sfer.

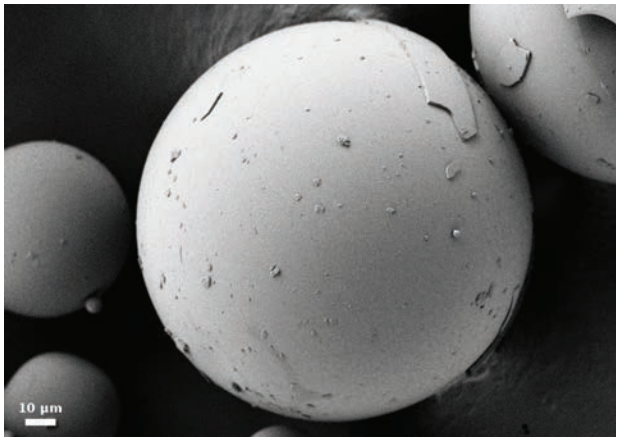

Fig. 2. SEM image of a single glass microsphere. Small fragments of other (broken) spheres can be seen on its surface.
Rys. 2. Obraz SEM pojedynczej mikrosfery szklanej. Na powierzchni widać niewielkie fragmenty innych, uszkodzonych sfer.

thickness was of the order of 1 µm. As the spheres were hollow, they could be easily damaged while handling and, consequently, many fragments of other spheres were present on their surfaces (Fig. 2).

All the deposition processes were conducted in a Picosun R200 Advanced ALD reactor. Trimethylaluminium [TMA, $(CH_3)_3Al$] was used as the Al precursor and nitrogen was the carrier gas. Aluminium oxide (Al_2O_3) was deposited by a thermal process with deionized water vapor employed as the oxygen precursor. In a different process, N_2 gas was flowing to the reactor chamber through a remote, inductively coupled RF plasma generator, where it was excited at ca. 2 MHz. This configuration should deliver a high concentration of charge-neutral plasma species to the substrate, allowing the deposition of aluminium nitride (AlN) layers. Alternate precursor pulses were always separated by flushing of the system with the carrier gas, argon being used to flush the plasma line.

An amount of approximately 200 mg of glass spheres was evenly spread over a 33 mm circular area of the reactor chuck, forming a ca. 2 mm thick powder-like layer with a surface density of the order of 20 mg/cm^2. The microspheres were placed in the reactor along with microscope slides (soda-lime glass). As the latter had a plane surface, they could be examined with a spectroscopic ellipsometer (Horiba UVISEL 2).

Both the spheres and the slides were imaged after deposition with a Carl Zeiss AURIGA CrossBeam Workstation scanning electron microscope (SEM). The spheres had to be glued on a carbon tape and covered with a thin layer of Au-Pd in order to reduce electrical charge accumulation. The glass slides were fractured to measure the thickness of the deposited layer.

The energy-dispersive X-ray spectroscopy (EDS) system of the SEM was used to analyze the chemical composition of the deposited layers but it was also employed to determine their thickness. This method requires a numerical model describing the interactions of electrons in the solid material. The model must take into account the mass density of the layer and substrate, the expected thickness range, and the SEM accelerating voltage. Such models were elaborated by performing Monte Carlo simulations of electron trajectories (using CASINO software). The ratios between EDS signals from elements expected in the deposited layer (in this case, Al) and in the substrate (Si) were then calculated from experimental spectra and fitted to the model, which yielded a thickness estimation. The above procedure was previously tested to give results consistent with spectral ellipsometry, notably for thin layers of Al_2O_3 on Si. A similar method is used in the ThinFilmID system, developed by Oxford Instruments [17].

3. Results and discussion

3.1. Aluminium oxide

After a series of preliminary ALD processes on Si and glass substrates, a temperature of 50°C was chosen, which was safe for the glass, high enough to be stabilized by the reactor heaters and resulted in an uniform Al_2O_3 deposition (Fig. 3). EDS mapping had confirmed that both deposited elements were present across the glass surface (Fig. 4). On both substrates, the refractive index of the oxide layer, determined by ellipsometry, had an average value of 1.57 at 633 nm wavelength. Deposition on the glass microspheres was therefore conducted at the same temperature.

After 200 cycles, the dielectric coating was not visible on a broad SEM image (Fig. 5) but a high-magnification (ca. 20 000x) micrograph of a broken sphere showed clearly the edge of the Al_2O_3 layer (Fig. 6). Many isolated low-profile objects, with a chemical composition similar to the deposited layer, were observed on the spheres sur-

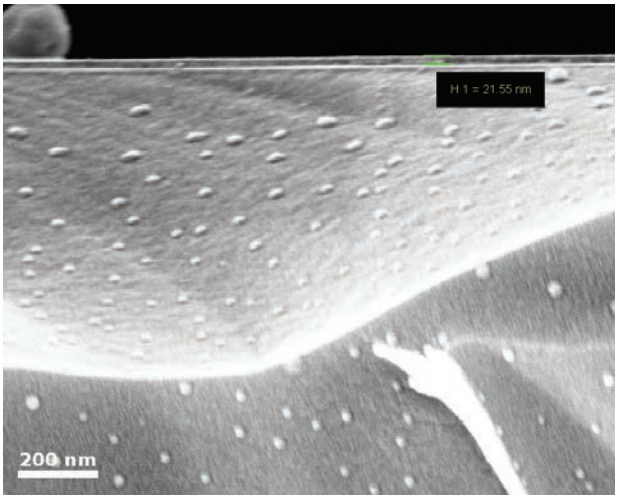

Fig. 3. SEM measurement of the Al_2O_3 layer on a fractured microscope slide after 200 deposition cycles. The imaging angle may cause a slight underestimation of the thickness.
Rys. 3. Pomiar SEM warstwy Al_2O_3 na przełomie płytki mikroskopowej po 200 cyklach osadzania. Kąt obrazowania może powodować lekkie zaniżenie grubości.

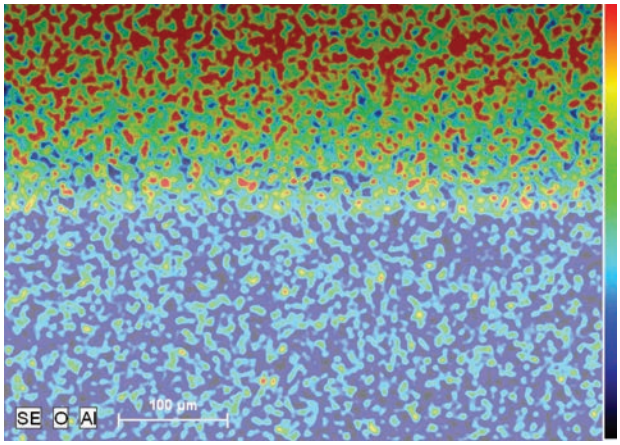

Fig. 4. Map of the summed intensity of EDS signals from Al and O after 400 deposition cycles. The upper part of the image corresponds to the oxide-covered surface of the microscope slide. The bottom part shows the glass fracture.
Rys. 4. Mapa rozkładu intensywności zsumowanego sygnału EDS pochodzącego od pierwiastków Al i O po 400 cyklach osadzania. U góry znajduje się powierzchnia płytki mikroskopowej pokryta warstwą tlenku, a niżej – przełom szkła.

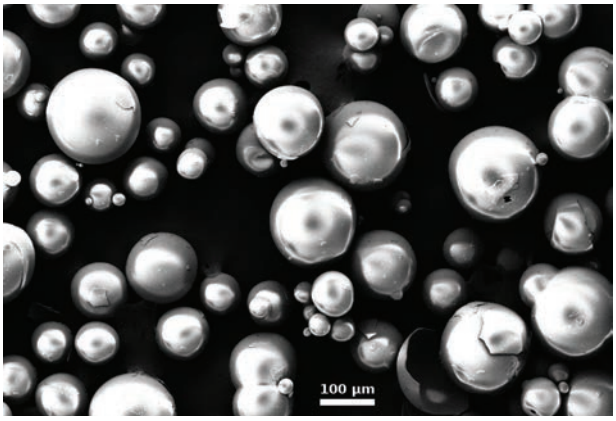

Fig. 5. Microspheres after depositing a 23 nm layer of Al_2O_3. Despite being covered with a thin conductive layer (Au-Pd), the spheres accumulate some electric charge, which results in apparent shadows on the SEM image.
Rys. 5. Mikrosfery po osadzeniu 23 nm warstwy Al_2O_3. Pomimo pokrycia cienką warstwą przewodzącą (Au-Pd), sfery gromadzą ładunek elektryczny z wiązki elektronów, co objawia się cieniami na obrazie SEM.

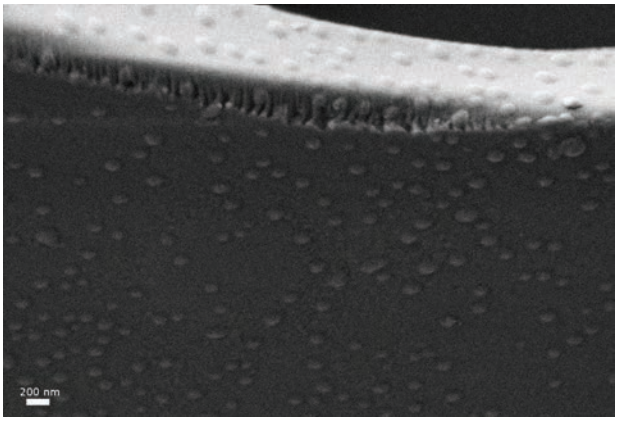

Fig. 6. Al_2O_3 layer visible on the surface of a broken sphere. The spots on the surface were identified as damage caused by the microscope electron beam, as they were appearing progressively with successive scans.
Rys. 6. Warstwa Al_2O_3 widoczna na powierzchni pękniętej sfery. Kropki na powierzchni zidentyfikowano jako uszkodzenia wywołane przez wiązkę elektronów mikroskopu, ponieważ pojawiały się stopniowo przy kolejnych skanowaniach.

face (Fig. 7). The absence of such objects on uncoated spheres, as well as their geometry, indicates these are Al_2O_3 crystallites.

In order to obtain layers of different thicknesses, the number of ALD cycles was varied between 175 and 800 cycles, which corresponds to deposition times from 90 minutes to nearly 7 hours. The layers deposited on glass slides were measured with ellipsometry, SEM imaging and EDS analysis. In one case, a crater with vertical walls (Fig. 8) was etched in the glass with a focused ion beam (FIB). The vertical section thus obtained appeared difficult to image because of strong electric charging from the SEM electron beam, which led to unsharp micrographs at higher magnifications. Additionally, the FIB etching itself had caused some blurring of the materials interface. Consequently, the measured Al_2O_3 thickness ranged from 85 to 120 nm but we assume that the measurement shown in Figure 9, close to 90 nm, is the most accurate. Direct measurements on the spheres were performed by analysis of EDS signal collected from a delimited area on the top of an individual sphere (Fig. 10). The thickness values thus obtained from 8 to 10 random spheres from one sample were then averaged (Fig. 11).

It appeared that 20 to 100 nm of dielectric was de-

posited in one process. The dependence between process length and Al_2O_3 thickness is shown in Fig. 12. It can be seen that the different measurement methods gave similar results but those obtained from the spheres (blue circles) are slightly higher and more linear with a growth rate of 1.2 Å per cycle.

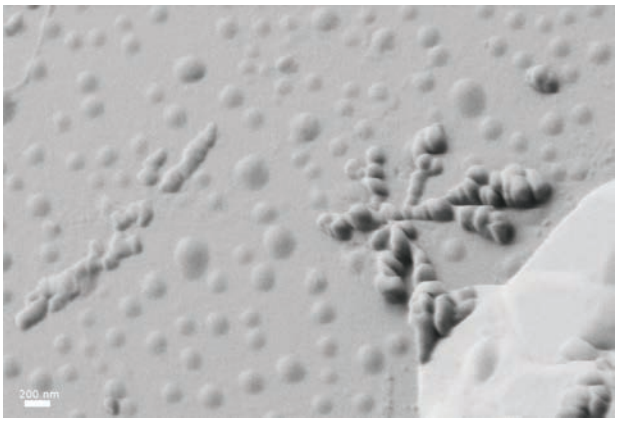

Fig. 7. An example of low-profile crystallite observed on a sphere surface after 175 Al_2O_3 deposition cycles.
Rys. 7. Przykład krystalitu o niewielkiej wysokości widocznego na powierzchni sfery po 175 cyklach osadzania Al_2O_3.

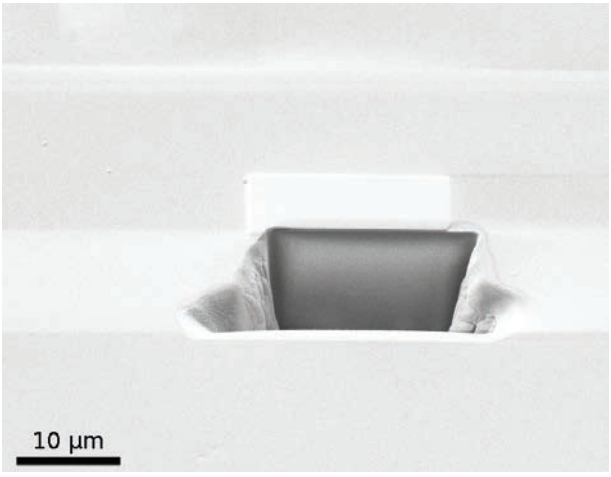

Fig. 8. A trapeziform FIB crater with vertical walls in a glass slide with an Al_2O_3 layer (800 deposition cycles). Prior to the ion etching, the sample had been covered with Au-Pd and, locally, also with platinum in order to avoid electrical charge accumulation and to protect the surface.
Rys. 8. Trapezowy krater z pionową powierzchnią w głąb materiału wytworzony poprzez trawienie jonowe (FIB) w płytce szklanej z warstwą Al_2O_3 (800 cykli osadzania). Przed trawieniem próbkę pokryto warstwą Au-Pd, a miejscowo także platyną, aby uniknąć gromadzenia się ładunku elektrycznego i zabezpieczyć powierzchnię.

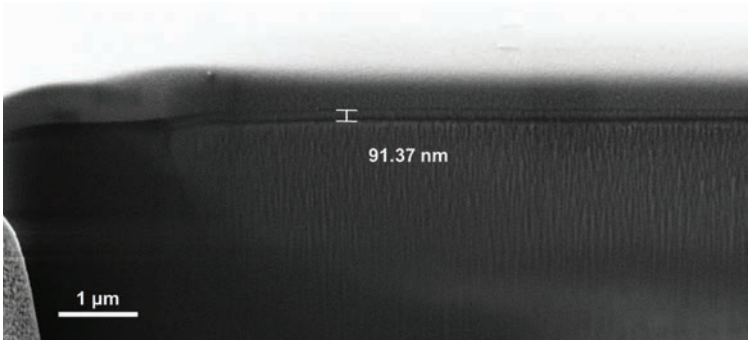

Fig. 9. SEM image of the FIB-etched section.
Rys. 9. Obraz SEM przekroju uzyskanego metodą FIB.

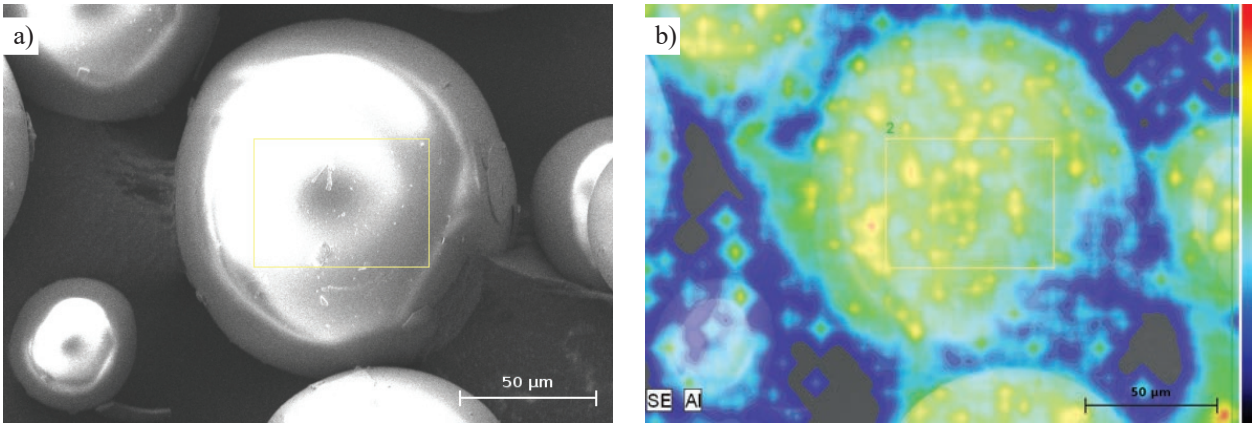

Fig. 10. a) SEM image of one of the microspheres chosen for thickness measurement after 200 cycles of Al_2O_3 deposition. The rectangular measurement area is indicated. b) Map of the intensity of EDS signal from Al measured in the same area. The average layer thickness determined for this sphere was 23.8 nm.
Rys. 10. a) Obraz SEM sfery wybranej do pomiaru grubości po 200 cyklach osadzania Al_2O_3. Zaznaczono prostokątny obszar pomiarowy. b) Mapa natężenia sygnału EDS od pierwiastka Al w tym samym obszarze. Dla tej sfery wyznaczono średnią grubość warstwy 23,8 nm.

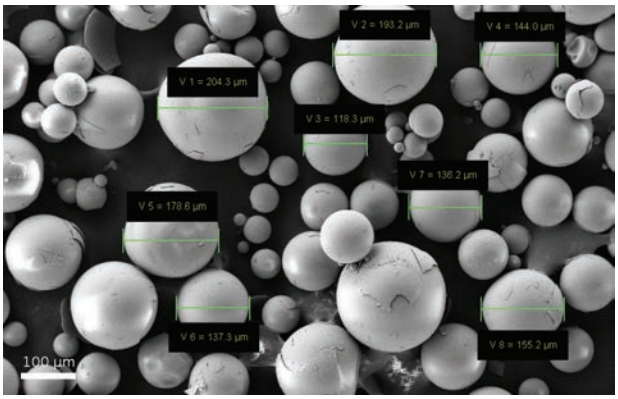

Fig. 11. SEM image with indicated diameters of random microspheres chosen for EDS thickness measurement after 175 Al_2O_3 deposition cycles. For spheres 1 to 8, the results of these measurements were, respectively: 28.5, 23.8, 23.0, 25.0, 24.7, 22.9, 25.9 and 19.0 nm. As the individual spheres undergo random rotations between oxide deposition and measurement, it can be assumed that the entire surface of each sphere was covered.

Rys. 11. Obraz z SEM z zaznaczonymi średnicami ośmiu przypadkowych mikrosfer wybranych do pomiaru grubości metodą EDS po 175 cyklach osadzania Al_2O_3. Dla sfer nr 1 do 8 pomiary te dały odpowiednio wyniki: 28,5; 23,8; 23,0; 25,0; 24,7; 22,9; 25,9 i 19,0 nm. Ponieważ poszczególne sfery ulegają przypadkowemu obróceniu w czasie między osadzaniem tlenku a pomiarem, można przyjąć, że została pokryta cała powierzchnia każdej z nich.

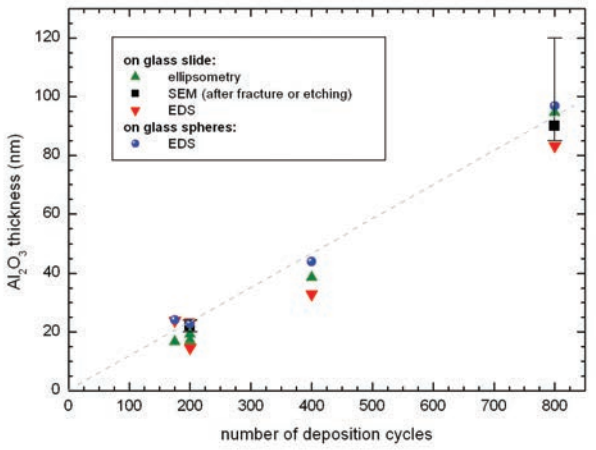

Fig. 12. Thicknesses of aluminium oxide obtained during five ALD processes at 50°C as a function of the process length. The SEM measurements were realized on the fractured surface of a glass slide for the 200-cycle process and on a FIB-etched section of a glass slide for the 800-cycle process. In both cases, the full range of the obtained values is shown along with their average.

Rys. 12. Grubości tlenku glinu uzyskane podczas pięciu procesów ALD w temperaturze 50°C w funkcji długości procesu. Pomiar SEM wykonano na przełomie płytki szklanej dla procesu o długości 200 cykli i na przekroju FIB płytki szklanej dla procesu o długości 800 cykli. W obu przypadkach zaznaczono wartość średnią i rozrzut otrzymanych wartości.

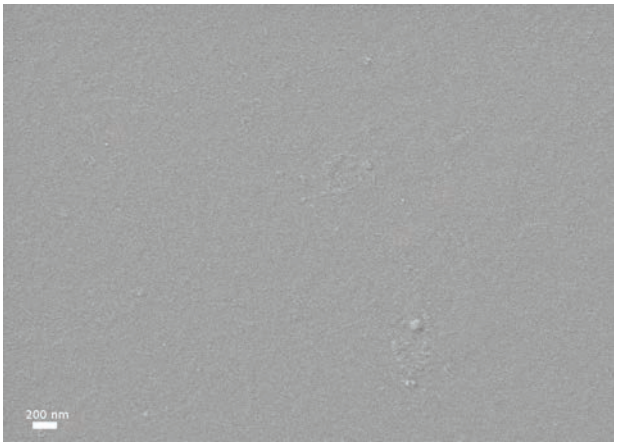

Fig. 13. SEM image of a glass slide with a 14 nm AlN layer after 177 deposition cycles. The surface has good uniformity with small (~10 nm) crystallites.

Rys. 13. Obraz SEM płytki szklanej z warstwą AlN o grubości 14 nm po 177 cyklach osadzania. Powierzchnia o dobrej jednorodności, z niewielkimi (~10 nm) krystalitami.

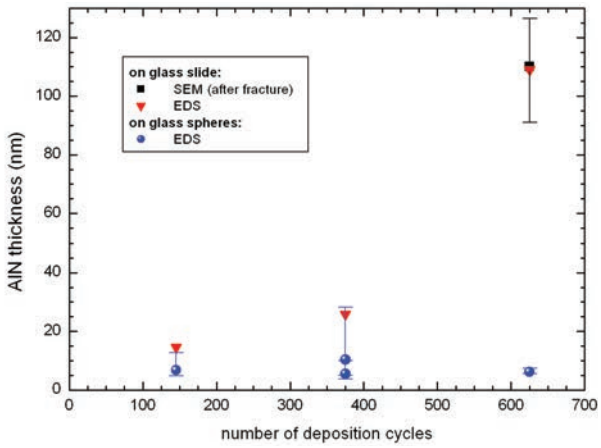

Fig. 14. Thicknesses of aluminium nitride obtained during four ALD processes, all of which were conducted at 150°C. The vertical bars show the full range of the observed values.

Rys. 14. Grubości azotku glinu uzyskane podczas czterech procesów ALD. Wszystkie wykonywano w temperaturze 150°C. Słupki pokazują zaobserwowany rozrzut grubości.

3.2. Aluminium nitride

In Ref. [18], a deposition temperature above 140°C and a H_2/N_2 plasma exposure time of at least 25 s were necessary to avoid the oxidation of AlN films after unloading from the ALD reactor. Similarly, in our study, an initial comparison of layers obtained at 100 and 150°C with pure N_2 plasma exposure times of 10 and 30 s showed that only the AlN deposited at the higher temperature and with the longer exposure time had a correct refractive index (1.8), a deposition rate of more than 0.8 Å per cycle and a good layer uniformity (Fig. 13). Subsequent processes were hence conducted using these parameters.

Fig. 14 shows the AlN layer thickness as a function of process length for processes from 145 to 625 cycles.

The use of plasma resulted in longer deposition cycles than for Al_2O_3, therefore these processes were taking up to 9.5 hours.

For glass slides, the energy selective backscattered (EsB) electron detector of the SEM microscope was useful for discerning the AlN layer from the fractured glass (Fig. 15). A wide range of thicknesses, from 14 to 110 nm, was obtained, with the average deposition rate reaching 1.8 Å per cycle at 625 cycles. On microspheres, however, the dielectric layer appeared to be very thin independently of the number of cycles. The EDS spectra were very different in both cases (Fig. 16) and the analysis showed that there is only 5 to 10 nm of AlN on most spheres.

Fig. 15. Imaging with the mass contrast EsB detector shows that the AlN layer on a glass slide is ca. 100 nm-thick after 625 deposition cycles.
Rys. 15. Obrazowanie detektorem kontrastu masowego EsB wskazuje, że warstwa AlN na płytce szklanej ma grubość około 100 nm po 625 cyklach osadzania.

It is known that AlN growth by chemical methods is highly sensitive to the presence of moisture, which should be eliminated from the reactor [19]. Nevertheless, a glass surface which is exposed to atmospheric air for an extended time will progressively adsorb water. A complete dehydration, i.e. removal of the physically adsorbed H_2O molecules, leaving only chemisorbed OH groups, occurs after heating to about 200°C [20], which exceeds our deposition temperature. The glass slides used in our experiment were subjected, shortly before deposition, to a cleaning procedure involving the use of acetone; however, no pretreatment was applied to the powder-like spheres. This leads us to assume that the limited growth observed on the latter substrates was caused by water or impurities present on their surface.

Groups of crystallites and irregular shapes were observed on the surface of all spheres. They were more numerous on spheres where the AlN thickness was lower than the average by EDS analysis (Fig. 17). Nevertheless, imaging with the EsB detector did not show any variations

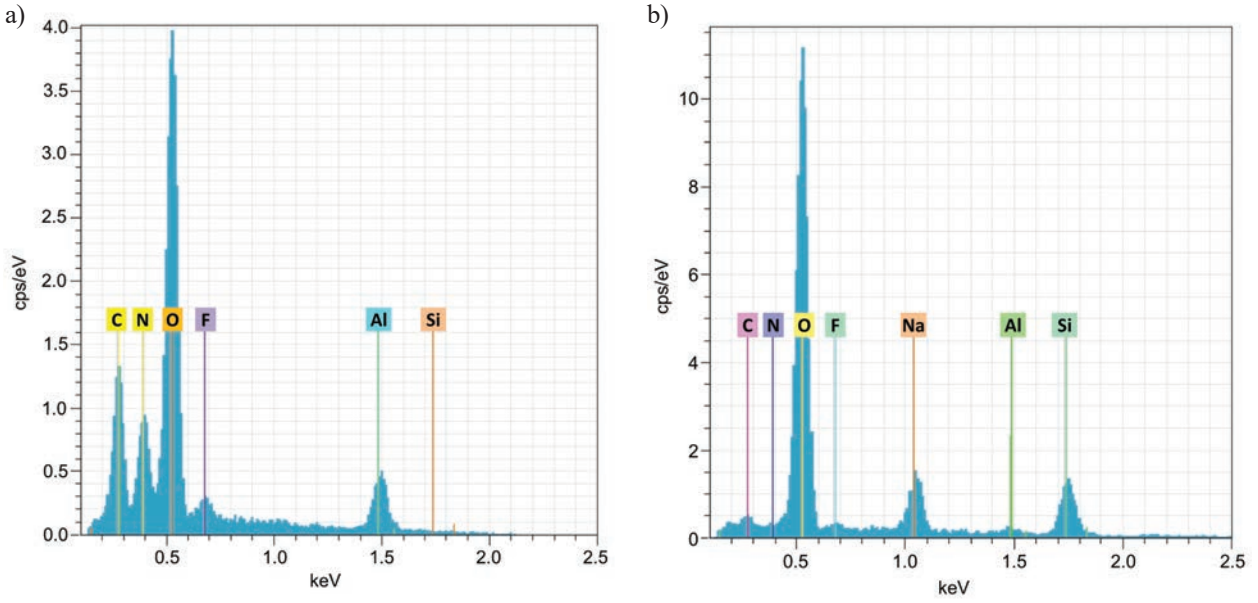

Fig. 16. EDS spectra obtained for the same deposition process and with the same measurement parameters (accelerating voltage 4 kV) a) from a glass slide. The absence of a peak from Si (contained in the glass) indicates it was suppressed by a thick AlN layer. (This peak can still be observed with different measurement parameters, which allows thickness calculation). b) from the surface of a sphere. The Si peak is very strong compared with the Al one, which indicates a very thin AlN layer.
Rys. 16. Widma EDS uzyskane dla tego samego procesu i tych samych parametrów pomiaru (napięcie przyspieszające 4 kV) a) z płytki szklanej. Brak widocznego piku od Si (zawartego w szkle) wskazuje na jego stłumienie przez grubą warstwę AlN. (Pik ten można jednak ujawnić przy innych parametrach pomiaru, co pozwala na obliczenie grubości). b) z powierzchni sfery. Pik Si jest bardzo silny w porównaniu z Al, co wskazuje na bardzo cienką warstwę AlN.

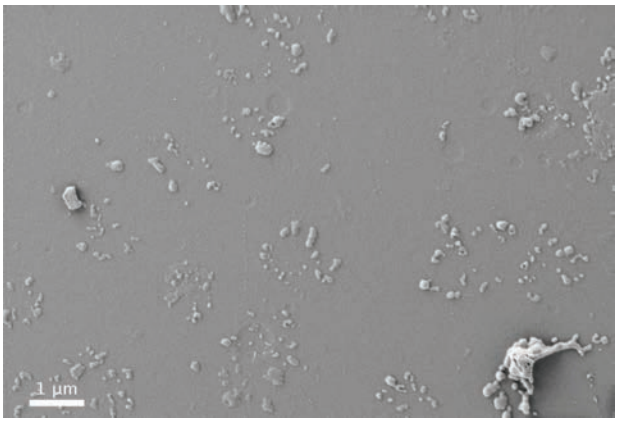

Fig. 17. SEM image of a microsphere surface after deposition of an AlN layer (375 deposition cycles). The thickness given by EDS analysis is 4 nm.
Rys. 17. Obraz SEM powierzchni mikrosfery po osadzeniu warstwy AlN (375 cykli osadzania). Grubość wyznaczona metodą EDS wynosi 4 nm.

in chemical composition across the surface, which proves that the AlN layer was continuous.

4. Conclusions

Aluminium oxide was deposited on glass microspheres by ALD at 50°C using TMA and H_2O as precursors. The experiment showed that, even on substrates with a highly curved surface, an arbitrary layer thickness can be obtained with good uniformity and repeatability. Still, the deposition of aluminium nitride at 150°C from TMA and pure N_2 plasma resulted in thin continuous layers. In both cases, EDS spectroscopy could be effectively used to assess the thickness of dielectric coating on substrates which are not plane at the microscale.

Acknowledgments

The authors would like to thank Krystyna Przyborowska and Beata Stańczyk for preparation of the glass and silicon substrates used in this study. The glass microspheres were provided by NGT Technology Sp. z o.o. (Działdowo, Poland).

References

[1] Budov V. V.: Hollow glass microspheres. Use, properties, and technology (Review), *Glass and Ceramics*, 1994, 51, 231 – 235

[2] Mao T., Tang Y., Mao J., Zhao R., Zhou Y.: Surface treatment for imparting solar-reflective thermal insulating properties to cellulosic paper, *International Journal of Biological Macromolecules*, 2018, 120, 1810 – 1816

[3] Zhang X., Wang P., Zhou Y., Li X., Yang E.-H., Yu T.X., Yang J.: The effect of strain rate and filler volume fraction on the mechanical properties of hollow glass microsphere modified polymer, *Composites Part B,* 2016, 101, 53 – 63

[4] Schnerch D., Dawood M., Rizkalla S., Sumner E., Stanford K.: Bond behavior of CFRP strengthened steel structures, *Advances in Structural Engineering*, 2006, 9, 805 – 817

[5] Kotnarowska D.: Kinetics of wear of epoxide coating modified with glass microspheres and exposed to the impact of alundum particles, *Progress in Organic Coatings*, 1997, 31, 325 – 330

[6] Psarski M., Celichowski G., Marczak J., Gumowski K., Sobieraj G. B.: Superhydrophobic dual-sized filler epoxy composite coatings, *Surface & Coatings Technology*, 2013, 225, 66 – 74

[7] Perfilov V. A., Oreshkin D. V., Semenov V. S.: Environmentally safe mortar and grouting solutions with hollow glass microspheres, *Procedia Engineering*, 2016, 150, 1479 – 1484

[8] Zhang Z., Wang K., Mo B., Li X., Cui X.: Preparation and characterization of a reflective and heat insulative coating based on geopolymers, *Energy and Buildings*, 2015, 87, 220 – 225

[9] Babić D., Burghardt T. E., Babić D.: Application and characteristics of waterborne road marking paint, *International Journal for Traffic and Transport Engineering*, 2015, 5, 150 – 169

[10] Xu J., Yang H., Yu Q., Chang L., Pang X., Li X., Zhu H., Li M., Zou G.: Synthesis and characterization of hollow glass microspheres coated by SnO_2 nanoparticles, *Materials Letters*, 2007, 61, 1424 – 1428

[11] Karches M., Morstein M., von Rohr P. R., Pozzo R. L., Giombi J. L., Baltanás M. A.: Plasma-CVD-coated glass beads as photocatalyst for water decontamination, *Catalysis Today*, 2002, 72, 267 – 279

[12] Sun L., Wan S., Yu Z., Wang L.: Optimization and modeling of preparation conditions of TiO_2 nanoparticles coated on hollow glass microspheres using response surface methodology, *Separation and Purification Technology*, 2014, 125, 156 – 162

[13] McAllister S. D., Patankar S. N., Cheng I. F., Edwards D. B.: Lead dioxide coated hollow glass microspheres as conductive additives for lead acid batteries, *Scripta Materialia*, 2009, 61, 375 – 378

[14] Pang X., Fu W., Yang H., Zhu H., Xu J., Li X., Zou G.: Preparation and characterization of hollow glass microspheres coated by $CoFe_2O_4$ nanoparticles using urea as precipitator via coprecipitation method, *Materials Research Bulletin*, 2009, 44, 360 – 363

[15] Fu W., Liu S., Fan W., Yang H., Pang X., Xu J., Zou

G.: Hollow glass microspheres coated with $CoFe_2O_4$ and its microwave absorption property, *Journal of Magnetism and Magnetic Materials*, 2007, 316, 54 – 58

[16] Groner M. D., Fabreguette F. H., Elam J. W., George S. M.: Low-temperature Al_2O_3 atomic layer deposition, *Chem. Mater*., 2004, 16, 639 – 645

[17] Giurlani W., Innocenti M., Lavacchi A.: X-ray microanalysis of precious metal thin films: thickness and composition determination, *Coatings*, 2018, 8, 84

[18] Goerke S., Ziegler M., Ihring A., Dellith J., Undisz A., Diegel M., Anders S., Huebner U., Rettenmayr M., Meyer H.-G.: Atomic layer deposition of AlN for thin membranes using trimethylaluminum and H_2/N_2 plasma, *Appl. Surf. Sci.*, 2015, 338, 35 – 41

[19] Perng Y.-C., Kim T., Chang J. P.: Effect of residual H_2O on epitaxial AlN film growth on 4H-SiC by alternating doses of TMA and NH_3, *Appl. Surf. Sci.*, 2014, 314, 1047 – 1052

[20] Zhuravlev L. T.: The surface chemistry of amorphous silica. Zhuravlev model, *Colloids and Surfaces A: Physicochemical and Engineering Aspects*, 2000, 173, 1 – 38